

Paper

Junction effects in St Venant's torsional stiffness

C. J. Burgoyne, MA, MSc, PhD, CEng, MStructE, MICE
Engineering Department, Cambridge University

Synopsis

A method is presented for dividing an open cross-section into components. Computer analyses have been undertaken to determine the effects of the junctions between components, which are significant in many sections. The results of these analyses are presented in the form of charts, which can be used in design offices to find equivalent sections whose inertia can be calculated by simple formulae. No computer analysis is needed by users of the charts.

The validity of the method is demonstrated by calculating the torsional stiffness of a Y-beam and its flange. The result is compared with accurate analyses, which have been used to calculate the torsional stiffness of the complete range of Y-beam sections.

Introduction

The calculation of St Venant's torsional stiffness for a complex open cross-section is not straightforward. Unlike the flexural stiffnesses, which are functions of simple integrals over the area of the section, the torsional stiffness depends on the solution of a differential equation which is valid over the whole cross-section. It is thus not normally possible to divide the section into a number of regions, for each of which the stiffness is known, and then to combine the results to accurately determine the properties of the overall section.

If it is required to calculate the torsional stiffness at present, the engineer must either solve the governing differential equation (which usually involves a complex numerical calculation) or make a number of simplifying assumptions which introduce errors of an unknown magnitude.

The commonest approximations make use of the well-known analytical solution for a rectangular section¹. This shows that the stiffness is a linear function of the shear modulus of the material (G), the largest dimension of the section (b), and the cube of the smallest dimension (t). The multiplying factor is a function of the aspect ratio, varying from 0.14 when $b = t$ to $\frac{1}{3}$ when $b \gg t$.

Estimates of the stiffness of more complex sections can be obtained by assuming that they are built up from a number of rectangles; the stiffness of each rectangle is determined taking account of its aspect ratio, and these stiffnesses are summed to give that of the whole section. A recent review paper by Johnson² studied most of the available methods. There are two disadvantages of this method that apply most significantly to concrete sections. It is not always obvious how best to divide the section into rectangles since sections may not have parallel sides and, with low aspect ratios, the choice of which is the 'long' side and which the 'short' side can cause significant changes in the results. Secondly, the torsional stiffness contributed by the junction areas can be much larger than that from the rectangular regions; Johnson² concluded that this was the most significant cause of error when estimating the torsional stiffness of concrete elements. The junction effect is particularly important when sections have chamfers and can cause serious underestimates of the torsional stiffness.

If individual rectangles have high aspect ratios, the error in the total stiffness is small; this is frequently the case with steel sections in which the breadth/thickness ratio for flanges and depth/thickness ratio of webs are usually of the order of 10:1 and 100:1, respectively. The thickening at junctions is not usually significant, so both errors mentioned above tend to be negligible. In addition, most steel members belong to standard ranges, so that an accurate 'once and for all' numerical calculation is carried out; the results are published along with other section properties.

Concrete sections, on the other hand, cause more problems. The aspect ratios of the components of the members are frequently less than 5:1, so that approximations which rely solely on dividing the section into a number of rectangles are not satisfactory. It is also much less likely that they are standard sections.

This paper presents a method by which the torsional stiffness of a complex section can be calculated without recourse to solving a complicated differential equation. All the numerical coefficients required will be provided

in the form of design charts for which all the complicated calculations have already been performed.

St Venant's theory

The derivation of the differential governing equation is well known and will not be repeated here. A stress function ψ must satisfy

$$\nabla^2 \psi = \frac{\partial^2 \psi}{\partial x^2} + \frac{\partial^2 \psi}{\partial y^2} = -2 \quad \dots (1)$$

over the cross-section, with ψ set to zero on the perimeter. The torsional inertia J is given by

$$J = 2 \int \psi \, dA \quad \dots (2)$$

and the maximum shear stress occurs where the slope of the stress function is a maximum. Hence

$$\tau_{\max} = \left(\frac{\partial \psi}{\partial n} \right)_{\max} \quad \dots (3)$$

Analytical solutions for this problem are not usually available for sections of practical interest; most solutions must be found numerically. Fig 1 shows contours of ψ for a precast Y-beam section with an *in situ* flange, calculated by an accurate finite difference method which is described below. The contours are at equal intervals in the value of ψ ; the particular values are of no concern here, but the complexity of the shape of the function is immediately apparent. The actual properties of these particular sections will be used as an example later in the paper.

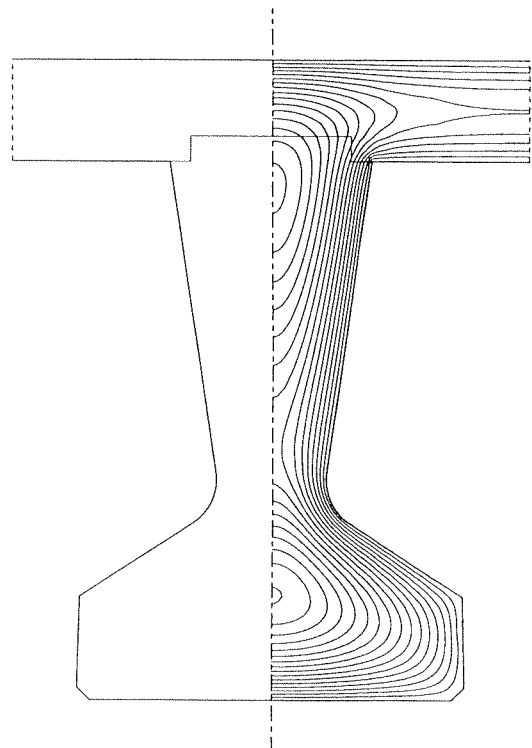


Fig 1. Contours of the stress-function ψ over a Y-5 beam with a 200 mm flange

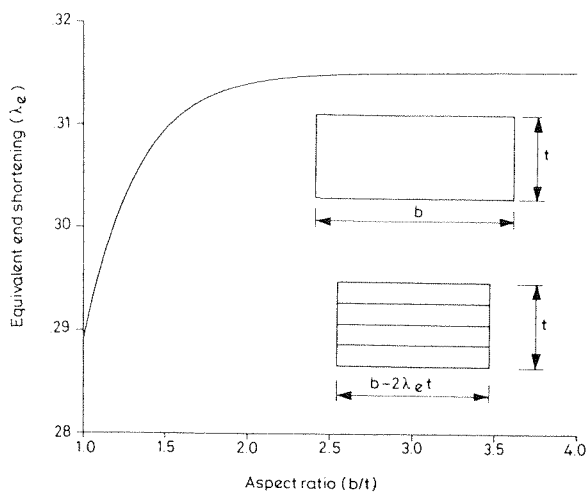


Fig 2. Rectangular section: reduction in length due to end effect

Rectangular section

One section for which an analytical solution does exist is the simple rectangular section shown in the inset in Fig 2. Timoshenko¹ gives the stress function, from which he obtains the torsional inertia

$$J = \frac{1}{3}bt^3 \left[1 - \frac{192}{\pi^5} \cdot \frac{t}{b} \cdot \sum_{n=1,3,5} \left(\frac{1}{n^5} \tanh \frac{n\pi b}{2t} \right) \right] \dots (4)$$

The first term represents the inertia of a rectangle with $b \gg t$, while the second term is a measure of the 'end effect', which is present for all rectangles, but is negligible at high aspect ratios.

It is postulated here that the end effect will be constant for aspect ratios larger than a certain (but as yet undetermined) value. It would be convenient if we could represent the real rectangular section by an equivalent member in which the end effects could be ignored. It will be assumed that the smaller dimension is unchanged, but that the larger dimension is reduced by $2\lambda_e t$, where λ_e is a function of the aspect ratio which we wish to determine.

Thus, the inertias of the equivalent sections will be given by

$$J = \frac{1}{3}(b - 2\lambda_e t) \cdot t^3 \dots (5)$$

which gives

$$\lambda_e = - \frac{96}{\pi^5} \sum_{n=1,3,5} \left(\frac{1}{n^5} \tanh \frac{n\pi b}{2t} \right) \dots (6)$$

The series converges rapidly; Fig 2 shows values of λ_e against the aspect ratio b/t . It can be seen that λ_e approaches an asymptote (.315124) as b/t gets larger, as expected. It should be noted how rapidly the asymptote is reached. When $b/t > 1.7$, λ_e is within 1% of the asymptote, and even at $b = t$ the difference is less than 9%.

The implication of this result is clear. It is possible to calculate the St Venant's constant of a rectangular section with great accuracy by assuming that the cross-section is reduced in length by $0.315t$ at each end, and then calculating the torsional inertia by ignoring the end effect completely. There is no need to solve a complex equation or to remember complex formulae.

When the aspect ratio b/t is 3, the value of λ_e is only trivially different from the result for an infinitely long section. Thus, if a section $1.5t$ long were analysed so that it satisfied eqn. (1), with the boundary condition at one end that ψ is prismatic, the correct distribution of ψ would result. This effect will be made use of later in the paper to decide what sections need to be analysed numerically.

The determination of λ_e by itself is relatively trivial; the answer is easily obtained by rearranging a well-known equation. But it points the way to a procedure for obtaining similar results for other components of a cross-section, which take account of the stiffening effects of the interaction between the various components by determining an 'equivalent section' whose stiffness can be determined by simple formulae.

For most sections it will not be possible to find suitable analytical solutions, analogous to that used for the rectangle. Thus, a numerical procedure will be needed to analyse the torsion eqn. (1) over a range of standard sections.

Computer program

A computer program was already available to solve the equations. The program was written for the work described in ref.3, where a full description is given.

The program uses finite differences and successive over-relaxation (SOR) to solve eqn. (1) subject to the appropriate boundary conditions. A rectangular grid of nodes is set up which covers the area of interest, and at every node within the section, a finite difference expression is set up which relates the value of the function at that node to the values at the four neighbouring points. At points on the boundary, the value of the function can be specified, which allows the boundary condition $\psi = 0$ to be specified; alternatively, the value of the slope of the function in either the x or the y direction can be fixed. This allows axes of symmetry to be specified (across which the slope must necessarily be zero) and also boundaries across which the function is presumed to be prismatic (when it will be specified that the slope is zero).

The equations that result from this finite difference representation would, if expressed in matrix form, have many elements that were zero. There would be only five non-zero elements on each row, three on or adjacent to the leading diagonal, and two outliers. The use of an iterative technique, such as SOR, to solve the equations allows only the non-zero elements to be stored, making the solution technique extremely efficient in computer memory. A penalty is paid in terms of execution time, but this is not significant. No problems have been found with non-convergence, which is potentially a problem with iterative techniques.

The format for the data input has been kept very flexible. This allows a wide range of sections to be considered without modifying the program. All of the results presented below have been obtained with the use of this program.

Tapering section

A partial analytical solution is available for a tapering section, but this will be seen not to be a complete solution due to the boundary conditions at the open end of the taper. For a long thin rectangular section, of thickness t (Fig 3(a)), the value of the stress function ψ varies parabolically, with a peak value of $t^2/4$ on the centreline. For a section with a taper half-angle of α (Fig 3(b)), which locally has a thickness t , the stress function can be shown to be increased by the factor $\mu = 1/(1-\tan^2 \alpha)$ over that of the rectangular section.

If the section tapers to a point, this function satisfies the boundary conditions identically along the edges, but clearly does not take into account the open end of the taper. This factor becomes dominant for large values of α ; indeed, at $\alpha = 45^\circ$, the factor becomes infinite, which indicates that the boundary conditions at the outer end become a dominant factor for large α and cannot be ignored. However, for low values of α , this function can be expected to be useful.

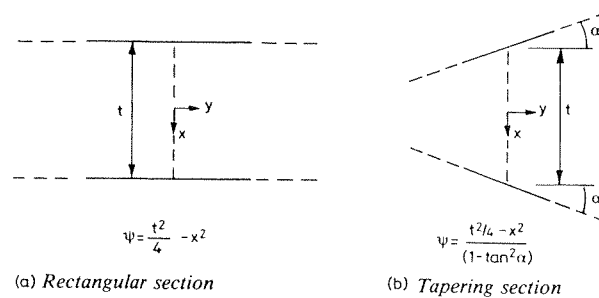


Fig 3. Stress function

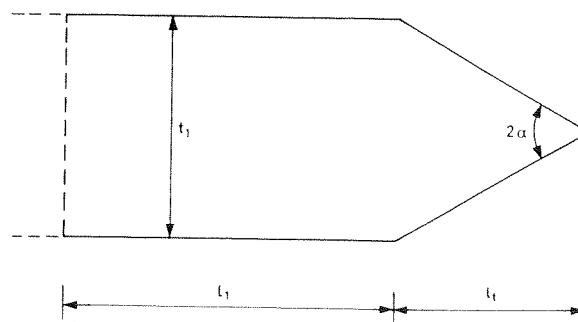


Fig 4. Tapering section analysed

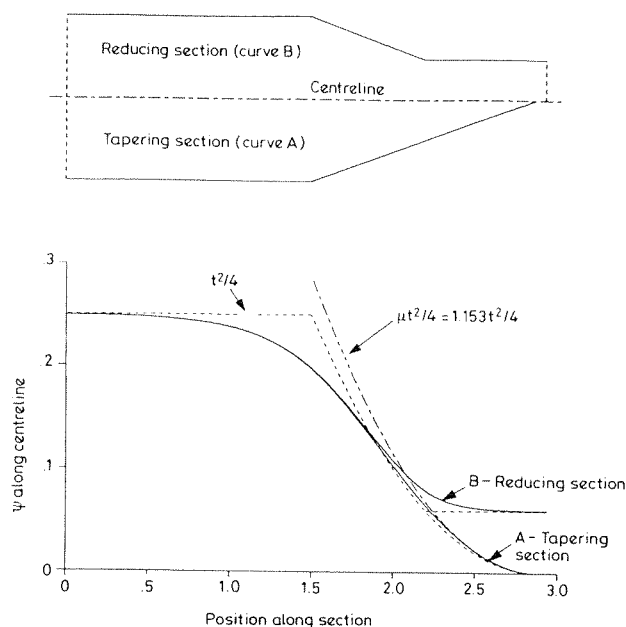


Fig 5. Tapering and reducing sections with $\alpha = 20^\circ$: values of ψ along the centreline

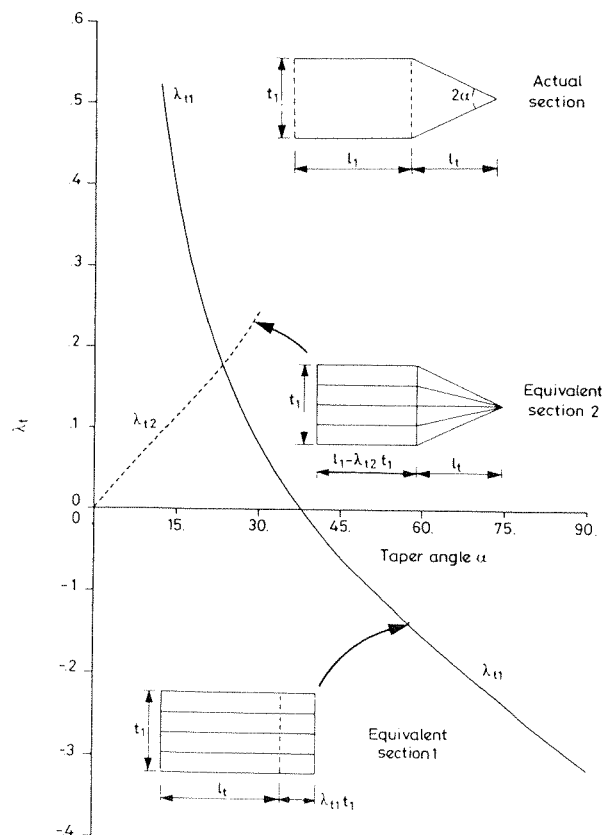


Fig 6. Taper section: alternative equivalent sections

To study these effects in more detail, consider a section which tapers from a thickness t_1 to zero over a length l_t (Fig 4). Integrating the analytical stress function discussed above, over the taper area, gives

$$J = \frac{t_1^3 l_t}{12(1 - \tan^2 \alpha)} = \frac{t_1^4}{24 \tan \alpha (1 - \tan^2 \alpha)} \quad \dots (7)$$

A number of sections of this type have been analysed using the computer program. The section extends for a length of $1.5t_1$ beyond the end of the

taper; at this end of the section, ψ is defined as being prismatic, as though the section continued indefinitely beyond this point. Extending the section in this way means that the results used here can be applied when the taper section forms part of a more complex shape.

Curve A in Fig 5 shows the value of ψ along the centreline of a taper section with $\alpha = 20^\circ$. Also shown on the figure are the value $t^2/4$ (the peak value to be expected in a rectangular section of thickness t) and $\mu t^2/4$ (the peak value expected in a taper section); for this section, $\mu = 1.153$. Near the point of the taper, the calculated value of ψ is close to this higher value, but soon becomes affected by the boundary conditions at the outer end. The value of ψ at the outer end, however, is very close to that expected in a prismatic section (even though only its normal slope was specified there), indicating that extending the section by $1.5t_1$ achieves the desired purpose.

An equivalent section is sought for which the torsional stiffness can be calculated by simple formulae and which has the same torsional stiffness as the real section when calculated by the program. Two alternatives seem logical, and are shown inset in Fig 6. In the first case, the taper is replaced by an equivalent length ($\lambda_{t1}t_1$) of prismatic rectangular section, for which

$$J = \frac{(l_t + \lambda_{t1}t_1)t_1^3}{3} \quad \dots (8)$$

λ_{t1} will be negative for large values of α , but positive for small values. This will be satisfactory for most values of α but, for very low α , values of λ_{t1} will be quite large.

An alternative for small α is to calculate J for the taper using eqn. (7), but to take account of the junction effect between the taper and the prismatic section by changing the length of the prismatic section by λ_{t2} . Thus,

$$J = \frac{t_1^4}{24 \tan \alpha (1 - \tan^2 \alpha)} + \frac{(l_t - \lambda_{t2}t_1)t_1^3}{3} \quad \dots (9)$$

These two expressions can be used with the results of the computer analysis of typical sections to calculate values of λ_{t1} and λ_{t2} . These are shown in Fig 6, which can now be used as a design chart. Care should be taken with the signs of these two correction factors. λ_{t1} can correspond to either an increase or decrease in length of the prismatic section, depending on α ; a positive value corresponds to an increase in length. λ_{t2} always corresponds to decreases in length, which are indicated by positive values in the chart.

Reducing section

These ideas can be extended to a reducing section of length l_t , where the width of the section tapers from t_1 to t_2 , with a taper angle α as before. As before, computer analyses have been carried out with the prismatic sections extending $1.5t_1$ and $1.5t_2$ away from the tapering section. Curve B in Fig 5 shows peak values of ψ for a section with $\alpha = 20^\circ$ and $l_t/t_1 = 0.7$. The length of the reducing section is too short for the end effects at the start and finish of the reducing section to be considered separately; values of ψ never follow the $\mu t^2/4$ curve predicted by the partial analytical solution. However, for smaller α , when l_t exceeds $t_1 + t_2$, the end effects would become independent.

For most sections, the reducing section (Fig 7(a)) is replaced with an equivalent length of the wider section λ_r , as shown in Fig 7(b). The torsional stiffness can then be calculated from

$$J = \frac{(l_t + \lambda_r)t_1^3}{3} + \frac{l_2 t_2^3}{3} \quad \dots (10)$$

Values of λ_r , derived from eqn. (10) and the computer analyses, are shown in Fig 8, which can be used for design purposes.

For small values of α , this is not entirely satisfactory. Instead, use can be made of the values of λ_{t2} derived earlier. Consider two sections; one narrows from a prismatic section of width t with angle α , the other widens from the prismatic section with the same angle. For small α the effect of the junction between the straight and tapered sections will be the same, but of opposite sign; for the narrowing section there will be a reduction in length by $\lambda_{t2}t$, while for the widening section there will be an increase in length by the same amount.

Thus, for the section reducing from t_1 to t_2 as in Fig 7(c), the St Venant's torsion constant can be found from

$$J = \frac{(l_t - \lambda_{t2}t_1)t_1^3}{3} + \frac{(t_1^4 - t_2^4)}{24 \tan \alpha (1 - \tan^2 \alpha)} + \frac{(l_2 + \lambda_{t2}t_2)t_2^3}{3} \quad \dots (11)$$

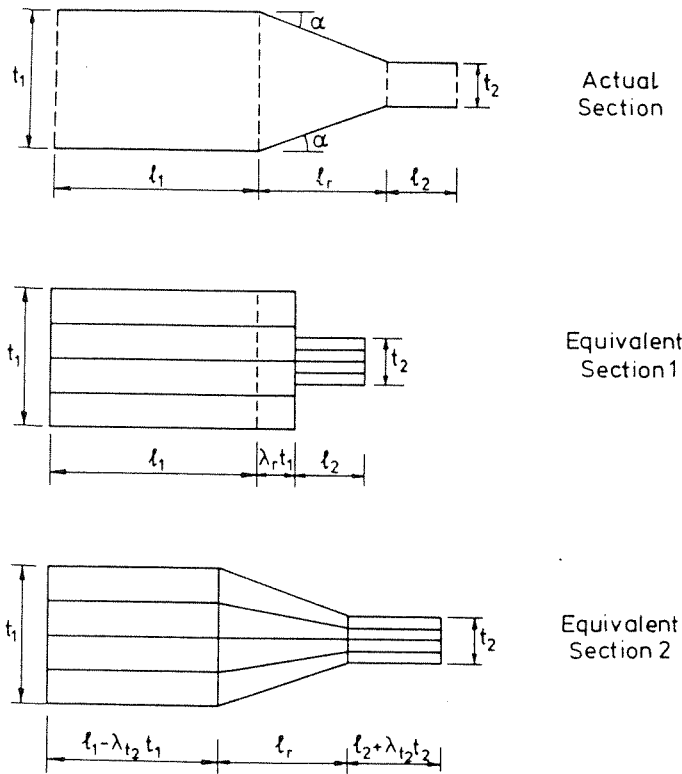


Fig 7. Equivalent sections for reducing section (the equivalent section 1 would normally be used for sections with a large taper angle, while equivalent section 2 would be used for sections with a shallow taper angle)

where λ_{t2} is found from Fig 6. The middle term of eqn. (11) relates to the tapering part of Fig 7(c), while the first and last term relate to the two parallel sections. There will be occasions when it is convenient to include these terms with adjacent regions.

The accuracy of the method can be seen by considering the section with $\alpha = 8^\circ$, $t_1 = 1.0$ and $t_r = 1.0$ (i.e. $t_2 = 0.7189$). From Fig 6, $\lambda_{t2} = -0.065$. Eqn. (11) gives $J = 0.83934$, while an accurate finite difference analysis gives $J = 0.83928$; the error is negligible.

Web-flange junction

The junction between a flange and a web which contributes significantly to the torsional stiffness of I- and T-sections, particularly if there are chamfers or radii at the resultant corners.

The finite difference program has been used to determine the torsional inertia of a section which includes the junction, the 45° chamfer (if it is present), and a length of the flange and web (1.5 times the appropriate thickness).

An equivalent section is sought which, if its inertia were calculated by the simple $(1/3)bt^3$ expression, would give the value that has been computed for the real section.

The equivalent sections chosen are shown inset in Figs 9 and 10. The length of the thicker component of the cross-section will be modified; thus, if $t_f \geq t_w$, the length of the flange will be increased by $\lambda_f t_f$ (Fig 9). Similarly, if the web is thicker than the flange, the web length will be increased by $\lambda_w t_w$ (Fig 10). This has the effect of keeping the modification factors λ_f and λ_w reasonably small. It is important to note that no chamfer is included in the equivalent cross-section; if it exists, its effects will be included in the values of the λ factors.

Figs 9 and 10 show values of λ_f and λ_w , respectively, plotted against the ratios of the flange and web thicknesses. Lines are plotted corresponding to different chamfer sizes (values of t_c/t_w). Two of the figures show more accurately the smaller values of λ_f and λ_w . The figures give results for sections with chamfer dimensions (t_c) less than the smallest of t_f and t_w . For larger chamfers, the triangular region defined by the chamfer becomes the dominant element in the torsional stiffness, and it is unreasonable to idealise the section as a simple rectangle.

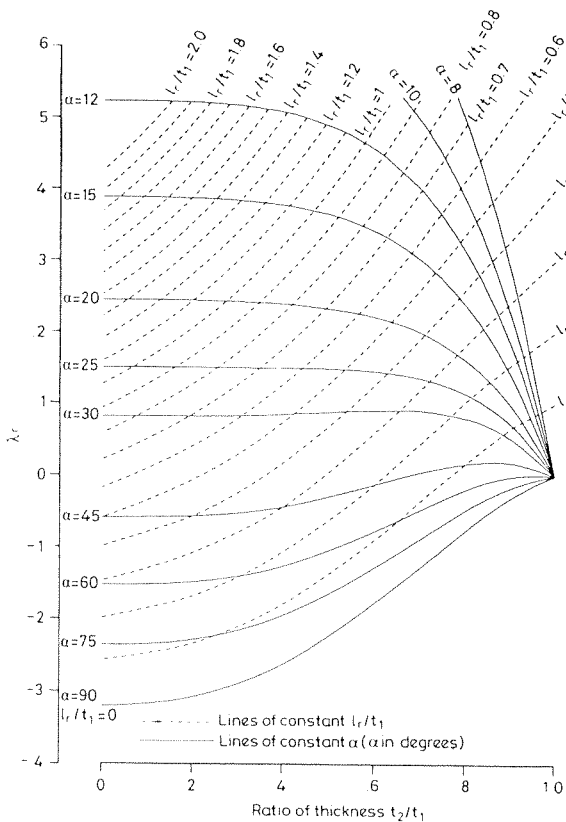


Fig 8. Design chart for reducing section, using the equivalent section 1 (Fig 7)

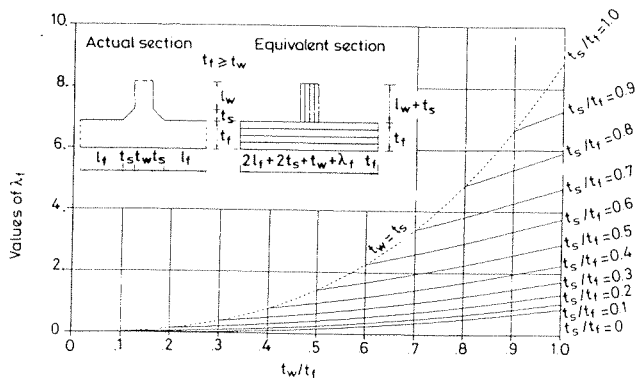


Fig 9(a). Equivalent section and design chart for T-junctions when $t_f > t_w$.

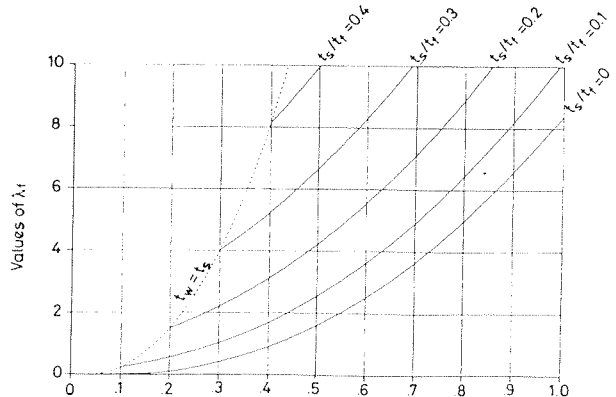


Fig 9(b). Design chart for $t_f > t_w$, for small λ_f

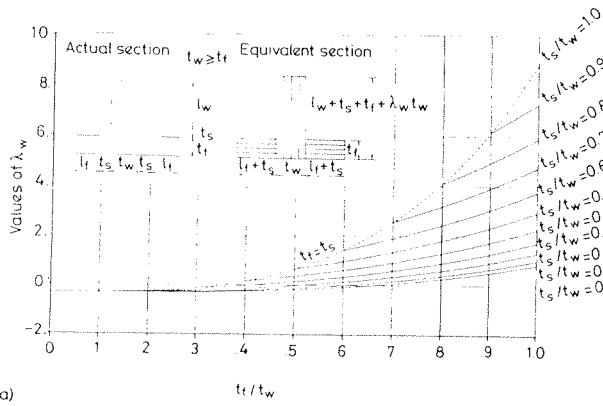


Fig 10(a). Equivalent section and design chart for T-junctions when $t_w > t_f$

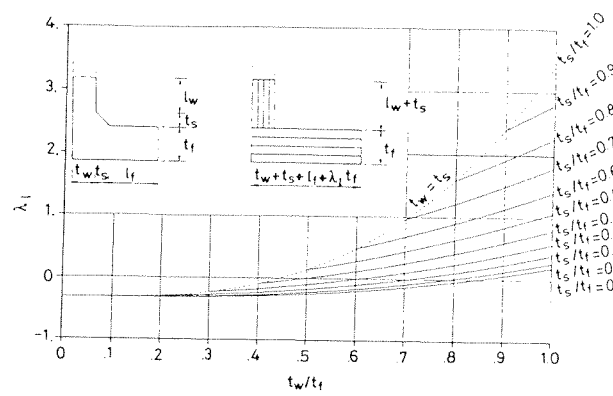


Fig 11(a). Equivalent section and design chart for L-junction

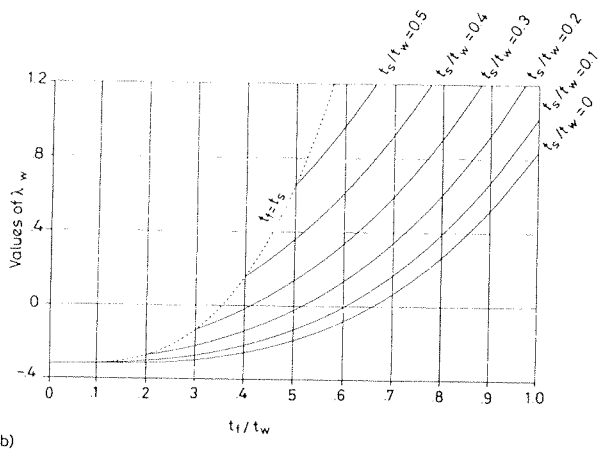


Fig 10(b). Design chart for $t_w > t_f$, for small λ_w

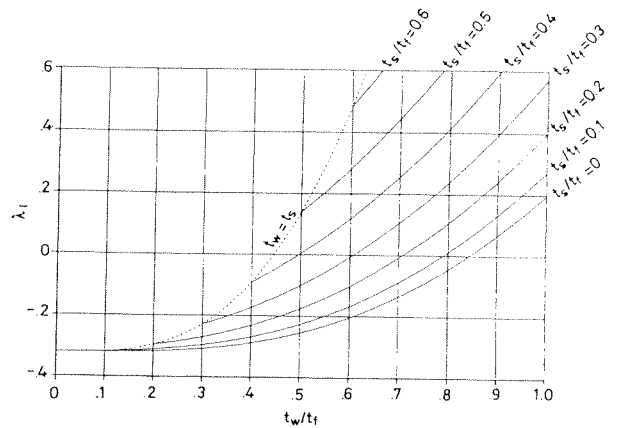


Fig 11(b). Design chart for L-junction, for small λ_1

L-junction

Certain sections will have L-shaped junctions between rectangular components. These can be catered for by a method similar to that used for the T-junction. In this case, the distinction between flange and web is irrelevant; the length of the thickest section (width t_f) will be modified by adding an equivalent length $\lambda_1 t_f$. Fig 11 shows values of λ_1 calculated for different sections.

Y-beam sections

As a separate exercise, the St Venant's torsional inertia of the new range of Y-beams, which has been proposed as the new standard bridge beam⁴, have been analysed using the computer program described earlier. It is from the results of one of these analyses that the contour plot of ψ shown in Fig 1 is taken. Eight beams are included in the Y-beam range (Fig 12), and they are designed to be used with a 200mm-thick top flange. Table 1 gives accurate values of the torsion constant for the eight beams acting alone and also with a 200mm-thick top flange of width 1 m that is presumed to continue to another beam. The flange clearly makes a significant contribution to the total torsional stiffness.

Use of the method

The Y-beams will be used to compare the results of an accurate analysis, given in Table 1, with the predictions of the method described in this paper. Consider the Y-5 section with a 200 mm flange. The section will be slightly idealised, as shown in Fig 13, thus ignoring the small corner splays and replacing the curved section at the throat with a short parallel section. Thus, from the top to the bottom, the section can be regarded as made up from:

- (a) two parallel flanges, length 303.2 mm, thickness 200 mm;
- (b) a T-junction between a flange of thickness 200 mm and a web of thickness 393.5 mm;
- (c) a section reducing in thickness from 393.5 mm to 216 mm, over a length of 615.5 mm ($\alpha = 8.204^\circ$);

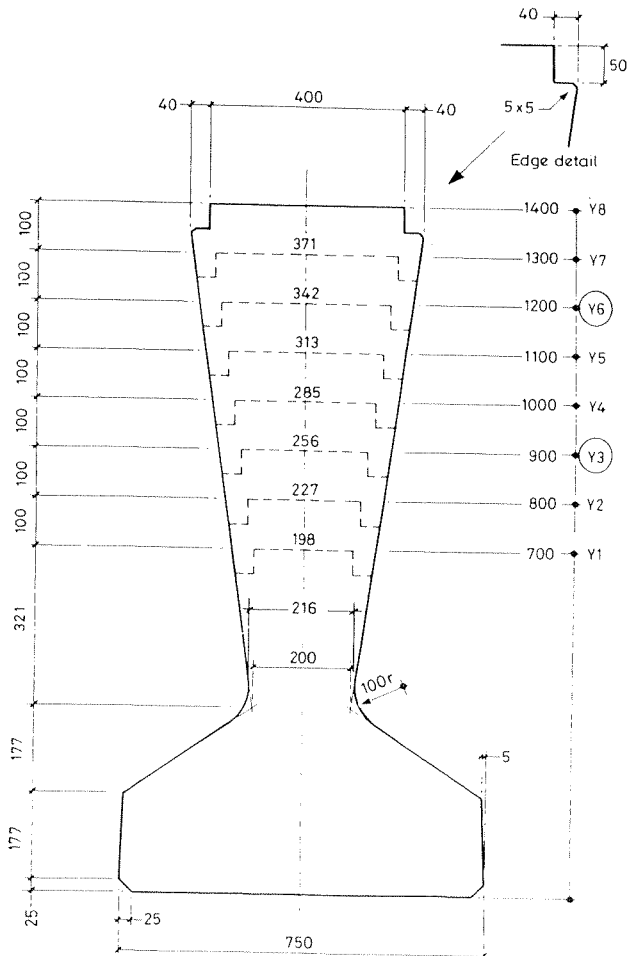


Fig 12. Y-beam sections (from ref.4)

- (d) a parallel section of length 60.7 mm and thickness 216 mm;
- (e) a T-junction between a web of thickness 216 mm and a flange of thickness 373.8 mm;
- (f) two flanges of reducing section, from 373.8 mm to 202 mm, over a length of 262 mm;
- (g) end sections at the extremes of each flange, of thickness 202 mm.

The contribution to the torsional stiffness of each of these components needs to be considered separately; numerical values and subtotals are shown in Fig 14.

- (a) The top flanges are parallel-sided elements, with no end effects, whose inertia can be calculated by a simple $bt^3/3$ calculation. There is no end effect at the outer ends, since the flange is assumed to continue into an adjacent beam, and at the inner end, the effect will be taken into account in (b).
- (b) The web coming in to the T-junction is thicker than the flange, so the length of the web is modified by λ_w taken from Fig 10(b). With $t_f/t_w = 0.508$, and $t_f/t_w = 0$, this gives $\lambda_w = -0.18$.
- (c) The reducing section has a relatively shallow taper angle (8.2°) and is best considered by the second method given for reducing sections. Thus the length of the thicker section will be reduced by $393.5\lambda_{t2}$, and the length of the thinner section is increased by $216\lambda_{t2}$, where λ_{t2} is found from Fig 6 to be 0.066. The torsional inertia of the tapering part of the section is found from the middle term of eqn. (11).
- (d) The throat is another short parallel-sided section.
- (e) The bottom junction is between a wider flange and a thinner web, so the length of the flange is adjusted by a factor λ_f , found from Fig 9(b) with $t_w/t_f = 0.577$, $t_f/t_f = 0$, which gives $\lambda_f = 0.22$.
- (f) The two bottom flanges are reducing sections with $t_2/t_1 = 0.540$, and $t_f/t_1 = 0.7$, so that λ_f from Fig 8 is 0.271. This use of the results for the symmetrically reducing section, on which Fig 8 is based, when applied to a section which is reducing on one side only, may be considered doubtful, but it is reasonable because skewing the section slightly will not significantly alter the values of ψ from which J is calculated.
- (g) The end effects at the end of each flange are taken into account by subtracting from the inertia of the section an amount equivalent to $\lambda_e t^3/3$ from the total inertia, where t in this case is taken as 202 mm.

The total inertia (obtained by summing the subtotals in Fig 14) is $.0188 \text{ m}^4$, which should be compared with the accurate result of $.01812 \text{ m}^4$ given in Table 1. The error is less than 4%, which would be acceptable for all practical purposes and is much better than could be achieved by simply replacing the section by a series of equivalent rectangles that do not take account of the junction effects.

It must be emphasised that this is a very severe test for this method. The method would give exact results for sections with parallel-sided elements between junctions, which are the ones most commonly used in construction as they are easy to form. The Y-beam section is exceptional in that respect because it is designed for production in factory conditions with moulds that are frequently reused, thus spreading the cost of the formwork over many beams.

Comparison with Johnson's results

Johnson² analysed a number of sections by a variety of methods which involve idealising the cross-section by a series of rectangles, with various methods of allowing for the junctions. As a reference, he used a finite element formulation to solve the governing differential equation. Table 2 shows the results of this finite element analysis and those of the present analysis. The nomenclature of the sections, and the units used, are the same as in ref.2. Johnson's section 2 has not been analysed, as there is clearly an error in Johnson's result; the section is an L-section, and the value he quotes is less than the inertia of the largest component of the L by itself, whereas it must be larger. His section 4 is also not included, as it includes '+' elements which are not analysed here.

The results can be seen to give very good agreement; the worst section is Jackson's (*sic*) exact I-section (quoted by Johnson²), which has large chamfers, with no parallel-sided elements in the flanges.

Limitations of the method

The method described here applies only to the calculation of the torsional inertia of open sections. Closed sections, which have a much higher torsional stiffness, have to have their inertias calculated by methods that take account of the hole(s) in the section. Shear flows have to be calculated around each hole, and additional equilibrium equations must be satisfied¹.

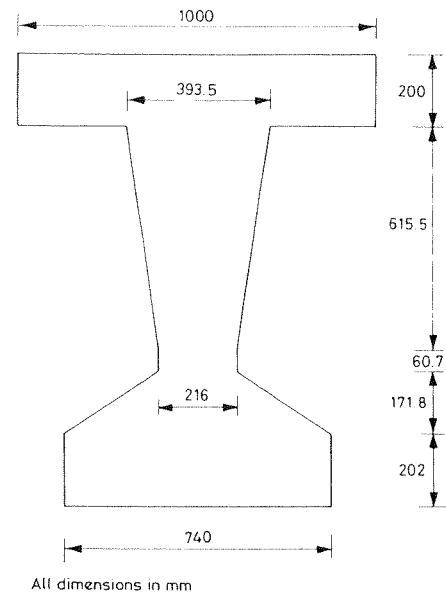


Fig 13. Idealised Y-5 section

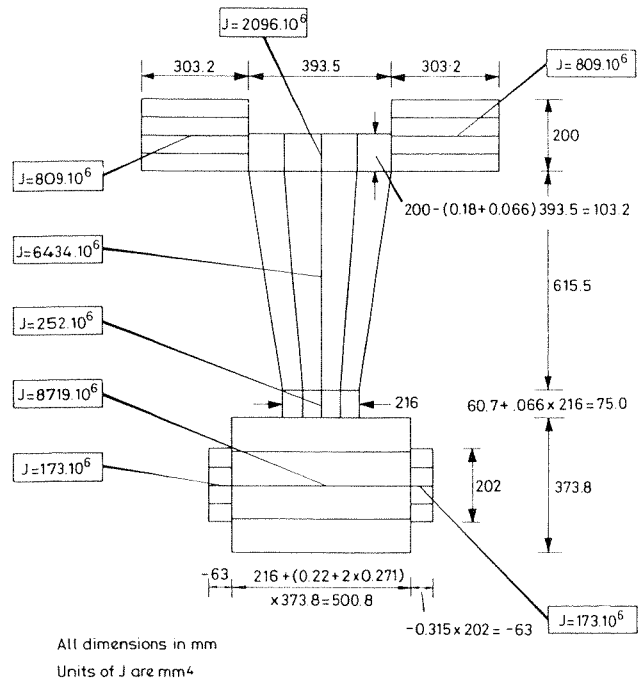



Fig 14. Equivalent Y-5 section, showing method of calculation of dimensions (see text for details of coefficients used)

TABLE 1 — Torsional inertia of Y-beams

Beam	Accurate torsional inertia (m ⁴)	
	Beam alone	Beam and flange
Y-1	.00860	.01235
Y-2	.00930	.01334
Y-3	.01019	.01460
Y-4	.01133	.01618
Y-5	.01277	.01812
Y-6	.01454	.02046
Y-7	.01670	.02328
Y-8	.01931	.02663

TABLE 2 — Comparison with Johnson's² analysis

Johnson's section	Johnson's fin. elem. result	Present analysis	Error %	Notes
1 (L-beam)	13.7	13.71	0	
3 	9.50	9.46	-0.4	(2'Ts' & 3'Ts')
Jackson 1 (idealised)	3920	3974	1.4	2'Ts' with no chamfers
Jackson 1 (exact)	4705	4976	5.7	2'Ts' with chamfers
Hambly 1 (exact)	72.4	74.5	2.9	2'Ts' with chamfers

The present analysis also applies only to uncracked sections. Thus it is probably relevant for prestressed concrete beams at the working load condition, but this covers the majority of cases when the transverse distribution of load is normally required. It is in this type of analysis that an accurate knowledge of the torsional stiffness is required. Cracking will clearly reduce the torsional stiffness. Regan⁵ estimated that the torsional stiffness of a Y-beam cracked in shear was about half the uncracked value, and more detailed results for prestressed I-beams were obtained by Luccioni *et al*⁶ while testing beams in combined torsion, flexure and shear.

For many concrete sections, the torsional warping stiffness also plays a significant part in resisting torsional loads, and this needs to be calculated by other means⁷.

Conclusion

A method has been presented which allows the St Venant's torsional inertia of a section to be determined by breaking the section up into a number of equivalent rectangles and tapering sections. The effects of junctions between elements of the cross-section, which significantly affect the torsional stiffness, are accounted for by adjusting the lengths of the parallel-sided elements by an amount that has been determined by an accurate computer analysis.

These length adjustments have been presented in the form of non-dimensional charts, which can then be used in design offices to find the inertia of most open sections, including thick-walled concrete sections, without the necessity of solving the stress function differential equation over the whole section.

It has been shown that the method gives good results, even for a section as complicated as a Y-beam, and it performed well when used on the examples given by Johnson.

References

1. Timoshenko, S. P., Goodier, J. N.: *Theory of elasticity*, chapter 10, 'Torsion', New York, McGraw Hill
2. Johnson, D.: 'The elastic torsional stiffness of concrete sections', *The Structural Engineer*, **69**, No. 11, 4 June 1991, pp207-210
3. Burgoyne, C. J.: 'Non-linear behaviour of beams and beam-columns', *PhD thesis*, University of London, 1982
4. Taylor, H. P. J., Clark, L. A., and Banks, C. C.: 'The Y-beam: a replacement for the M-beam in beam and slab bridges', *The Structural Engineer*, **68**, No. 23, 4 December 1990, pp459-465
5. Regan, P. E.: 'Behaviour of precast, prestressed Y-beams in shear, torsion and negative bending', *The Structural Engineer*, **68**, No. 23, 4 December 1990, pp466-473
6. Luccioni, B. M., Reimundin, J. C., and Danesi, R. F.: 'Prestressed concrete I-beams under combined mixed torsion, flexure and shear', *Proc. ICE*, Part 2, **91**, 1991, pp577-592
7. Waldron, P.: 'Sectorial properties of straight thin-walled beams', *Computers & Structures*, **24**, 1986, pp147-156